Non-local two-dimensional turbulence and Batchelor's regime for passive scalars

By S. NAZARENKO[1] AND J.-P. LAVAL[2]

[1]Mathematics Institute, University of Warwick, Coventry, CV4 7AL, UK

[2]CEA/DAPNIA/SAp L'Orme des Merisiers, 709, 91191 Gif sur Yvette, France

We study small-scale two-dimensional non-local turbulence, where interaction of small scales with large vortices dominates in the small-scale dynamics, by using a semi-classical approach developed in Dyachenko, Nazarenko & Zakharov (1992), Nazarenko, Zabusky & Scheidegger (1995), Dubrulle & Nazarenko (1997) and Nazarenko, Kevlahan & Dubrulle (1999). Also, we consider a closely related problem of passive scalars in Batchelor's regime, when the Schmidt number is much greater than unity. In our approach, we do not perform any statistical averaging, and most of our results are valid for any form of the large-scale advection. A new invariant is found in this paper for passive scalars when their initial spectrum is isotropic. It is shown, analytically, numerically and using a dimensional argument, that there is a spectrum corresponding to an inverse cascade of the new invariant, which scales like k^{-1} for turbulent energy and k^1 for passive scalars. For passive scalars, the k^1-spectrum was first found by Kraichnan (1974) in the special case of advection δ-correlated in time, and until now it was believed to correspond to an absolute thermodynamic equilibrium and not a cascade. We also obtain, both analytically and numerically, power-law spectra of decaying two-dimensional turbulence, k^{-2}, and passive scalar, k^0.

1. Introduction

Formation of coherent large-scale vortices from turbulence is a common place in two-dimensional numerical simulations of the Euler/Navier–Stokes equations (Smith & Yakhot 1993; Borue 1993, 1994; McWilliams 1984; Benzi *et al.* 1986; Benzi, Patnello & Santangelo 1987; Babiano *et al.* 1987; Santangelo, Benzi & Legras 1989; McWilliams 1990; Brachet, Meneguzzi & Sulem 1986; Brachet *et al.* 1988 and Kevlahan & Farge 1997), as well as in laboratory experiments (Couder 1984; Sommeria 1985; Cardoso, Marteau & Tabeling 1994, 1995). The intensity of the coherent vortices grows via the inverse energy cascade and eventually they start producing a significant feedback on turbulence. At this moment, the low-wavenumber spectrum changes from its transient Kolmogorov shape, $k^{-5/3}$ (for forced turbulence), to a steeper spectrum; see Smith & Yakhot (1993), Borue (1994). There is no consensus in literature on how the non-local interaction with large-scale vortices affects the small-scale spectrum in both forced and decaying turbulence. Computations of McWilliams (1984) (decaying turbulence, 128^2 grid, hyperviscosity), Benzi *et al.* (1986, 1987) (decaying turbulence, 128^2 to 512^2 resolution, hyperviscosity), Babiano *et al.* (1987) (forced turbulence, 128^2) and Santangelo *et al.* (1989) (decaying turbulence 1024^2 with hyperviscosity) indicate

steeper than k^{-3} spectra. McWilliams suggested that the coherent vortices suppress the enstrophy cascade by the coherent vortices which explains steeper than k^{-3} spectra in small scales (McWilliams 1984, 1990). On the other hand, numerical experiments of Brachet *et al.* (1986) and Brachet *et al.* (1988) (decaying turbulence, resolution up to 2048^2), Borue (1994) (forced turbulence, resolution up to 1024^2) show the k^{-3} energy spectrum of small-scale turbulence. The difference in the considered regimes and, perhaps, differences in performance of the numerical methods may explain the discrepancy. Ohkitani (1991) used the Weiss criterion (Weiss 1991) to decompose the vorticity field into the coherent structures and 'background'. He showed numerically that the background field possesses the k^{-3} energy spectrum whereas the coherent structures are characterized by a steeper spectrum. A similar conclusion was recently reached by Kevlahan & Farge (1997) who used wavelets, and who showed that the coherent structures, although very sparse, contain most of the turbulent energy. In spite of these achievements in the numerical simulation of two-dimensional turbulence, the underlying physical mechanisms of the turbulence-vortex interactions still remain unclear.

To study the interaction of turbulence with coherent large-scale vortices we consider an extreme case where these interactions are dominant in the turbulence evolution and local interactions between the small scales may be neglected. This case will be referred to as *non-local turbulence*. It is reasonable to think that two-dimensional turbulence becomes non-local at late stages of its evolution when much of the energy is condensed into the largest scale of the system. A simple estimate shows that the spectrum must decay more steeply than k^{-3} at large scales for the non-local turbulence to be stronger than the local in the small scales. High-resolution numerical simulations of forced turbulence by Borue (1993) indicate that the enstrophy transfer is strongly non-local. It is of course an open question whether or not the local interactions can ever be negligible in a real experiment. However, the study of such a pure non-local interaction is important as it is the opposite extreme to the classical Kolmogorov picture, in which the non-local interactions are neglected with respect to the local ones. The truth, then, should be expected in between these two extremes. Remarkably, as we shall see in this paper, the non-local theory predicts the same k^{-3}-spectrum as the local theory does which makes this spectrum quite universal.

A formalism suitable for description of the non-local two-dimensional turbulence was developed in Dubrulle & Nazarenko (1997). In that paper, the scale separation between the small turbulence scale and the large vortex scale was used to average the Euler equations over the small scales and derive a coupled system of equations for the small-scale and large-scale components. Note that no averaging is made over the large scales. For the small-scale component this approach leads to a semi-classical (WKB) description, where the wavepackets of turbulence are advected by the mean flow, and their wavenumber is evolving due to the local mean strain/shear produced by the large vortices. The enstrophy of the turbulence wavepackets is conserved whereas the energy is not: it can be transferred to (or be drawn from) the large-scale vortices. In turn, turbulence produces a feedback on the large-scale flow via the averaged Reynolds stress. The equations for the small and large scales form a complete system of equations called the two-fluid model. The original idea of the two-fluid model was proposed for β-plane turbulence in Dyachenko, Nazarenko & Zakharov (1992) and it was later applied to modelling of sound–vortex nonlinear interactions in Nazarenko, Zabusky & Scheidegger (1995), modelling of rapid distortion of three-dimensional turbulence by inhomogeneous strain in Nazarenko, Kevlahan & Dubrulle (1999) and for developing a new subgrid model for two-dimensional turbulence in Laval, Dubrulle & Nazarenko (1999).

In this paper we consider the small-scale turbulence to be initially isotropic and homogeneous (for decaying turbulence) or to be generated by an isotropic and homogeneous forcing (for forced turbulence). Applications where the scale separation approach gives rigorous results exist but of course are very limited. For example, one can think of a suddenly introduced forcing at a scale which is much less than the integral scale. In this case, our approach will be rigorous until the spectral gap is filled. However, we will go beyond such limited applications and will show that some of the effects found under the scale separation assumption will survive when the gap is filled (e.g. the k^{-3}-spectrum) whereas the other results become harder to verify but they allow the formulation of quite an important hypothesis about the long time asymptotics in forced two-dimensional turbulence.

Generally, the small-scale turbulence feeds back onto the large scales affecting their long-time evolution. Such a feedback was included in the model developed in Dyachenko *et al.* (1992). Dubrulle & Nazarenko (1997), Nazarenko *et al.* (1995, 1999) and Laval (1999). It is interesting that the feedback term appears to be very small when the initial small-scale turbulence (or the turbulence forcing) is statistically isotropic; in fact it is identically equal to zero in our model as was shown in Nazarenko *et al.* (1999). Thus, the large-scale vortex dynamics completely decouples from the small-scale turbulence, and the mean velocity field can be considered as an external field for the small-scale dynamics. This result, together with the fact that the small-scale vorticity is advected unchanged by the mean velocity field, makes the dynamics of initially isotropic turbulence identical to the passive-scalar advection problem. Therefore, we shall consider the turbulence and the passive-scalar spectra in parallel in this paper. The analogy between the small-scale vorticity and passive scalars is not new, see e.g. Kraichnan (1975). Babiano *et al.* (1987) argued, however, that because of the turbulence feedback on the coherent vortices the small-scale turbulence dynamics is very different from the passive-scalar dynamics. Again, in our case such a feedback is absent because of the non-locality and initial isotropy and homogeneity of turbulence.

For passive scalars, the reason for the non-locality (scale separation) is completely different from the case of turbulence. It arises, for example, if the Schmidt number is much greater than unity, so that much smaller scales are present in the passive scalar than in the advecting flow. The case of the small-scale passive scalar advected by a large-scale flow was first studied by Batchelor (1959), and it is referred to as Batchelor's regime. The statistical behaviour of passive scalar in Batchelor's regime has been studied in great detail by Chertkov *et al.* (1995). In the present paper, we do not perform any statistical averaging over large scales. This allows us to show that some passive-scalar properties are general for any large-scale flow and independent of its statistics and to show the sensitivity of some other properties to the particular location in the large-scale flow.

An important result which we are going to use in this paper is that the energy of initially isotropic turbulence is conserved; it is neither transferred to nor is it drawn from the large-scale flow as in the general case of anisotropic initial turbulence, see Nazarenko, *et al.* (1999). Consequently, there is a new spectrum associated with an inverse spectral flux of energy, k^{-1}. Together with the enstrophy-flux spectrum, the energy-flux spectrum can be derived from a dimensional argument, as well as obtained numerically and as an asymptotic analytical solution in the two-fluid model.

It is well known that the k^{-3} enstrophy-cascade spectrum has a k^{-1} analogue among the passive-scalar spectra; see Kraichnan (1975). The k^{-1} passive-scalar spectrum was first found by Batchelor (1959). Importantly, the new k^{-1} energy spectrum obtained

in this paper also has its analogue in the passive-scaler-dynamics k^1-spectrum. The k^1-spectrum is a special case of the k^{D-1}-spectrum (where D is the number of dimensions) obtained by Kraichnan (1974) for the passive scalar in Batchelor's regime with a velocity field δ-correlated in time. Kraichnan noticed that the k^{D-1}-spectrum corresponds to equipartition of the passive scalar among all degrees of freedom and concluded that this spectrum corresponds to a state of absolute statistical equilibrium. In this paper we show that although the passive scalar is indeed uniformly distributed among wavenumbers for the k^1-spectrum, this spectrum corresponds to the cascade of another passive-scalar invariant, and, therefore, describes a state which is very far from the statistical equilibrium. Moreover, we show that Batchelor's k^{-1} passive scalar cascade spectrum corresponds to a wavenumber equipartition of the new invariant, which means that the situation is completely symmetric and both k^1- and k^{-1}-spectra belong to the same class. The new invariant is found in this paper and called pseudo-energy because in the two-dimensional case it is analogous to the energy of turbulence. The pseudo-energy cascade is inverse, and the corresponding k^{D-1}-spectrum is formed on the low-wavenumber side of the forcing scale, as verified numerically in this paper.

We also consider the case of freely decaying turbulence, for which we obtain, both analytically and numerically, a k^{-2}-spectrum. Correspondingly, for free decay of passive scalar we obtain a k^0-spectrum.

This paper is organized as follows. We derive the equations describing the evolution of the small-scale turbulence and describe the numerical method used to compute these equations in §2. Section 3 is devoted to finding the turbulence spectra and their asymptotic behaviour for decaying turbulence. A similar study for forced turbulence is presented in §4. We show how to use the dimensional analysis to obtain the spectral exponents for the non-local turbulence in §5. In §6 we re-interpret our results for the passive scalar advection problem. We also consider the passive scalar problem for an arbitrary number of dimensions in this section and we find a new invariant for the passive scalars. We summarize our results in §7.

2. Dynamics of non-local turbulence

2.1. *Derivation of the basic equations*

Let us write the two-dimensional Navier–Stokes equations formulated in terms of vorticity ω as

$$\omega_t + \boldsymbol{u} \cdot \nabla \omega = \nu \nabla^2 \omega, \tag{2.1}$$

where $\boldsymbol{u}$ is the velocity. Consider the turbulent vorticity at small scales l and suppose that the turbulence is non-local, that is that only non-local interactions with large scales L, such that

$$\epsilon = l/L \ll 1, \tag{2.2}$$

are important for the turbulence dynamics at scale l. There are several equivalent ways that lead to the semi-classical description of the small-scale turbulent dynamics in this case, for example using the Wigner function (Dyachenko *et al.* 1992; Dubrulle & Nazarenko 1997), the partial Fourier transform (Nazarenko *et al.* 1995) or the Gabor transform (Nazarenko *et al.* 1999). Here we shall use the Gabor transform of vorticity ω defined as

$$\hat{\omega}(\boldsymbol{x}, \boldsymbol{k}, t) = \int f(\epsilon^* |\boldsymbol{x} - \boldsymbol{x}_0|) \mathrm{e}^{\mathrm{i}\boldsymbol{k} \cdot (\boldsymbol{x} - \boldsymbol{x}_0)} \omega(\boldsymbol{x}_0, t) \, \mathrm{d}\boldsymbol{x}_0, \tag{2.3}$$

where $k \sim 2\pi/l$, $1 \gg \epsilon^* \gg \epsilon$ and $f(x)$ is a function rapidly decreasing at infinity, for example e^{-x^2}.

Define the averaging as

$$\bar{\boldsymbol{u}}(\boldsymbol{x}, t) = \int f^2(\epsilon^* |\boldsymbol{x} - \boldsymbol{x}_0|) \boldsymbol{u}(\boldsymbol{x}_0, t) \, d\boldsymbol{x}_0, \tag{2.4}$$

where f is the same function as in the Gabor transform (2.3), and, therefore, the averaging is over a length which is intermediate between the small scale l and the large scale L. The non-locality of turbulence means that the dominant contribution to the advecting velocity field comes from the large scales,

$$|\boldsymbol{u} - \bar{\boldsymbol{u}}| \ll |\bar{\boldsymbol{u}}|. \tag{2.5}$$

Note that this condition does not require that the small-scale vorticity be small compared to the large-scale vorticity. Inequalities (2.2) and (2.5) make a complete set of applicability conditions for our theory.

Let us apply the Gabor transform to the vorticity equation (2.1) and use condition (2.5),

$$\partial_t \hat{\omega} + \int f(\epsilon^* |\boldsymbol{x} - \boldsymbol{x}_0|) e^{i\boldsymbol{k} \cdot (\boldsymbol{x} - \boldsymbol{x}_0)} \nabla_0 \cdot (\bar{\boldsymbol{u}}(\boldsymbol{X}_0) \, \omega(\boldsymbol{x}_0)) \, d\boldsymbol{x}_0 = -\nu k^2 \hat{\omega}, \tag{2.6}$$

where ∇_0 denotes the gradient with respect to $\boldsymbol{x}_0$. Because of the decreasing kernel f, the main contribution into the integral here comes from $|\boldsymbol{x} - \boldsymbol{x}_0| \sim 1/\epsilon^*$. Therefore, one can Taylor expand function $\bar{\boldsymbol{u}}$ which varies significantly only at the large scale $1/\epsilon \gg 1/\epsilon^*$. Neglecting the quadratic terms in this Taylor expansion, which are small as $(\epsilon/\epsilon^*)^2$, we have

$$\partial_t \hat{\omega} + \int f(\epsilon^* |\boldsymbol{x} - \boldsymbol{x}_0|) e^{i\boldsymbol{k} \cdot (\boldsymbol{x} - \boldsymbol{x}_0)} \nabla_0 \cdot (\bar{\boldsymbol{u}}(\boldsymbol{x}) \, \omega(\boldsymbol{x}_0)) \, d\boldsymbol{x}_0$$

$$+ \int f(\epsilon^* |\boldsymbol{x} - \boldsymbol{x}_0|) e^{i\boldsymbol{k} \cdot (\boldsymbol{x} - \boldsymbol{x}_0)} \nabla_0 \cdot [((\boldsymbol{x}_0 - \boldsymbol{x}) \cdot \nabla) \bar{\boldsymbol{u}}(\boldsymbol{x})] \, \omega(\boldsymbol{x}_0) \, d\boldsymbol{x}_0 = -\nu k^2 \hat{\omega}. \tag{2.7}$$

Integrating by parts and changing $\nabla_0 \to -\nabla$ in the first integral in (2.7), we see that this integral is equal to $(\bar{\boldsymbol{u}} \cdot \nabla) \hat{\omega}$. Integrating by parts the second integral and changing $(\boldsymbol{x}_0 - \boldsymbol{x}) \to i\partial_{\boldsymbol{k}}$ and $\nabla_0 \to i\boldsymbol{k}$, we have for the second term $-(\nabla(\bar{\boldsymbol{u}} \cdot \boldsymbol{k})) \cdot \partial_{\boldsymbol{k}} \hat{\omega}$. Thus, one can write the equation for $\hat{\eta}$ as follows:

$$D_t \hat{\omega} = -\nu k^2 \hat{\omega}, \tag{2.8}$$

where

$$D_t = \partial_t + \dot{\boldsymbol{x}} \cdot \nabla + \dot{\boldsymbol{k}} \cdot \partial_{\boldsymbol{k}},$$
$$\dot{\boldsymbol{x}} = = \bar{\boldsymbol{u}}, \tag{2.9}$$
$$\dot{\boldsymbol{k}} = -\nabla(\boldsymbol{k} \cdot \bar{\boldsymbol{u}}). \tag{2.10}$$

Equations (2.9) and (2.10) are called the ray equations. Let us introduce the Jacobi matrix Λ such that

$$\Lambda_{ij} = \partial_{x_j} a_i, \quad i, j = 1, 2, \tag{2.11}$$

where $\boldsymbol{a}(\boldsymbol{x}, t) = (a_1, a_2)$ is the initial coordinate; it is an inverse function to the solution of (2.9). In terms of Λ the solution of (2.10) is (Nazarenko *et al.* 1999)

$$\boldsymbol{k} = \nabla(\boldsymbol{q} \cdot \boldsymbol{a}) = \Lambda^T \boldsymbol{q}, \tag{2.12}$$

where Λ^T is transposed Λ and q is the initial wavenumber.

Because of the fluid incompressibility, $\mathrm{d}\boldsymbol{x} = \mathrm{d}\boldsymbol{a}$, we have

$$\det \Lambda = 0. \tag{2.13}$$

From this condition and (2.12) it follows that the motion is also incompressible in the wavenumber space,

$$\mathrm{d}\boldsymbol{k} = \mathrm{d}\boldsymbol{q}. \tag{2.14}$$

Below we shall be interested in finding the turbulence spectra in the inertial range where the viscosity is negligible. Neglecting the viscosity term in (2.8) we can find the solution to the equation

$$\hat{\omega}(\boldsymbol{x}, \boldsymbol{k}, t) = \hat{\omega}(\boldsymbol{a}, \boldsymbol{q}, 0). \tag{2.15}$$

2.2. *Conservation laws*

Note that $N = \int |\hat{\omega}|^2 \, \mathrm{d}\boldsymbol{k}$ is the $\boldsymbol{x}$-density of the small-scale enstrophy. It follows from (2.15) and (2.14) that the enstrophy density is conserved on the mean-flow trajectory

$$N_t + \overline{\boldsymbol{u}} \cdot \nabla N = 0. \tag{2.16}$$

One can show (Nazarenko *et al.* 1999) that for initially isotropic turbulence the energy density

$$E(\boldsymbol{x}, t) = \int \frac{|\hat{\omega}(\boldsymbol{x}, \boldsymbol{k}, t)|^2}{k^2} \, \mathrm{d}\boldsymbol{k}, \tag{2.17}$$

is also conserved on the mean-flow trajectory in the inviscid range,

$$E_t + \overline{\boldsymbol{u}} \cdot \nabla E = 0. \tag{2.18}$$

Both the energy and enstrophy conservation laws play an important role in the dynamics of the turbulence. Below, we shall be interested in the energy spectrum of the turbulence defined as

$$E(\boldsymbol{x}, k, t) = \int \frac{|\hat{\omega}(\boldsymbol{x}, \boldsymbol{k}, t)|^2}{k} \, \mathrm{d}\theta, \tag{2.19}$$

where θ is the polar angle in the wavenumber space.

2.3. *Numerical method*

All analytical results obtained in this paper are verified and illustrated throughout using numerical simulations. Our numerical method to compute non-local turbulence is based on equation (2.15) according to which $\hat{\omega}$ is conserved along the trajectories in $(\boldsymbol{k}, \boldsymbol{x})$-space given by the solutions of (2.9) and (2.10). Therefore, we represent the initial enstrophy field $\hat{\omega}(\boldsymbol{k}, \boldsymbol{x}, 0)$ by a large ensemble of M particles each carrying a small enstrophy σ and having initial coordinates and wavenumbers $\boldsymbol{a}_j$ and $\boldsymbol{q}_j$ respectively,

$$|\hat{\omega}(\boldsymbol{x}, \boldsymbol{k}, 0)|^2 = \sum_{j=1}^{M} \sigma \, \delta(\boldsymbol{k} - \boldsymbol{q}_j) \, \delta(\boldsymbol{x} - \boldsymbol{a}_j). \tag{2.20}$$

Then for $t > 0$ the wavenumber-coordinate enstrophy distribution will be given by

$$|\hat{\omega}(\boldsymbol{x}, \boldsymbol{k}, t)|^2 = \sum_{j=1}^{M} \sigma \, \delta(\boldsymbol{k} - \boldsymbol{k}_j(t)) \, \delta(\boldsymbol{x} - \boldsymbol{x}_j(t)), \tag{2.21}$$

where $\boldsymbol{x}_j(t)$ and $\boldsymbol{k}_j(t)$ have to be found by solving the equation for particle trajectories (2.9) and (2.10) with initial conditions $\boldsymbol{x}_j(0) = \boldsymbol{a}_j$ and $\boldsymbol{k}_j(0) = \boldsymbol{q}_j$. To find the spectra

one has to integrate this distribution over the coordinate volume, which is equivalent to the summation over the particles in our case.

This method is similar to the particle-in-cell (PIC) method to compute the Vlasov equation in plasma physics. The first discussion of using PIC to compute small-scale turbulence was given in Dyachenko *et al.* (1992) in the context of β-plane dynamics. The large-scale flow was computed by a standard pseudo-spectral method with hyperviscosity. We used the large-scale fields generated at resolutions 128^2 and 256^2 and different kinds of hyperviscosities to ensure that the resolution is sufficient for our results to be robust and insensitive to the specific choice of these numerical parameters. A more detailed description of our numerical method can be found in Laval *et al.* (1999).

3. Freely decaying turbulence

Let us consider first the simplest case where the initial spectrum is concentrated on a circle in k-space and homogeneous in x-space,

$$|\hat{\omega}(x, k, 0)|^2 = \frac{N}{2\pi q_0} \delta(k - q_0), \tag{3.1}$$

where q_0 is a number. We will also assume that initially the small-scale spectrum is separated from the large-scale turbulence by a gap in k-space, and we will study the evolution of the small-scale component for the times until this spectral gap is filled by intermediate scales. Because the equations for the small-scale turbulence are linear, the generalization to the any isotropic initial spectrum is obtained by simply integrating over the rings of type (3.1). From (2.15),

$$|\hat{\omega}(x, k, t)|^2 = |\hat{\omega}(a, q, 0)|^2 = \frac{N}{2\pi q_0} \delta(q - q_0), \tag{3.2}$$

where $a = a(x, t)$ and $q = q(x, k, t)$ are the initial position and initial wavenumber correspondingly. Substituting this expression into (2.19) we have

$$E(x, k, t) = \frac{N}{2\pi q_0 k} \int_0^{2\pi} \delta(q - q_0)\,\mathrm{d}\theta = \frac{N}{2\pi q_0 k |\partial_\theta q|} = \frac{N}{\pi k |\partial_\theta q^2|}. \tag{3.3}$$

Here, q^2 must be expressed in terms of k and θ, and θ must be eliminated using the condition $q = q_0$. From (2.12) and $\det \Lambda = 0$ we have an expression for q in terms of k,

$$q_x = -\Lambda_{12}k_x + \Lambda_{11}k_y, \quad q_y = \Lambda_{22}k_x - \Lambda_{21}k_y. \tag{3.4}$$

Thus

$$q^2 = q_x^2 + q_y^2 = (-\Lambda_{12}k\cos\theta + \Lambda_{11}k\sin\theta)^2 + (\Lambda_{22}k\cos\theta - \Lambda_{21}k\sin\theta)^2$$
$$= k^2(c + c_1\cos 2\theta - c_2\sin 2\theta) = k^2(c + c_3\sin(\gamma - 2\theta)), \tag{3.5}$$

where

$$c_1 = (\Lambda_{22}^2 + \Lambda_{12}^2 - \Lambda_{11}^2 - \Lambda_{21}^2)/2, \tag{3.6}$$

$$c_2 = \Lambda_{11}\Lambda_{12} + \Lambda_{21}\Lambda_{22}, \tag{3.7}$$

$$c = (\Lambda_{22}^2 + \Lambda_{12}^2 + \Lambda_{11}^2 + \Lambda_{21}^2)/2, \tag{3.8}$$

$$c_3 = \sqrt{c_1^2 + c_2^2}, \tag{3.9}$$

$$\gamma = \arctan(c_1/c_2). \tag{3.10}$$

From $q^2 = q_0^2$ we find

$$\sin(\gamma - 2\theta) = \frac{q_0^2}{c_3 k^2} - c/c_3. \tag{3.11}$$

Further,

$$|\partial_\theta q^2| = 2c_3 k^2 |\cos(\gamma - 2\theta)| = 2c_3 k^2 \sqrt{1 - \sin^2(\gamma - 2\theta)} = 2k^2 \sqrt{c_3^2 - (q_0^2/k^2 - c)^2}. \tag{3.12}$$

Using the definitions of c_1, c_2, c_3 and c and the condition $\det \Lambda = \Lambda_{11}\Lambda_{22} - \Lambda_{21}\Lambda_{12} = 1$ one can verify by a lengthy but simple calculation that $c_3^2 - c^2 = -1$, and therefore

$$|\partial_\theta q^2| = 2k^2 \sqrt{2cq_0^2/k^2 - q_0^4/k^4 - 1}. \tag{3.13}$$

Substituting this expression into (3.3) we finally have

$$E(\boldsymbol{x}, k, t) = \frac{N}{2\pi k^3 \sqrt{2cq_0^2/k^2 - q_0^4/k^4 - 1}}. \tag{3.14}$$

It is easy to check that

$$\int E(\boldsymbol{x}, k, t)\, \mathrm{d}k = \frac{N}{q_0^2} = \text{const},$$

which is a manifestation of the more general result that for any isotropic spectrum the energy is constant on the fluid trajectory (Nazarenko *et al.* 1999).

3.1. *Large-time asymptotics of $E(\boldsymbol{x}, k, t)$*

First, the spectrum $E(\boldsymbol{x}, k, t)$ is finite only in a limited range of wavenumbers, $k_{min} < k < k_{max}$, where k_{min} and k_{max} are to be found from the condition that the quadratic expression under the square root in (3.14) is equal to zero,

$$k_{min}^2 = q_0^2(c - \sqrt{c^2 - 1}), \tag{3.15}$$
$$k_{max}^2 = q_0^2(c + \sqrt{c^2 - 1}). \tag{3.16}$$

Note that $c = 1$ and $k_{min} = k_{max} = q_0$ at $t = 0$. Second, the spectrum is infinite at $k = k_{min}$ and $k = k_{max}$. These two observations are natural if we keep in mind that the initial circle distribution in k-space becomes an ellipse, see (3.11). One can see from (3.15) and (3.16) that the ellipse area is constant,

$$S = \pi k_{min} k_{max} = \pi q_0^2. \tag{3.17}$$

This gives a useful relation between k_{min} and k_{max},

$$k_{min}/q_0 = q_0/k_{max}. \tag{3.18}$$

The aspect ratio of the ellipse is

$$\lambda = k_{max}/k_{min} = k_{max}^2/q_0^2 = c + \sqrt{c^2 - 1}. \tag{3.19}$$

Expressing c in terms of λ gives

$$2c = \lambda + 1/\lambda. \tag{3.20}$$

The value of k_{max}, and therefore λ, increases with time because of the large-scale distortion (shearing/straining). We shall consider in more detail in the Appendix how fast this growth is. (Of course, all the results about the aspect ratio growth discussed
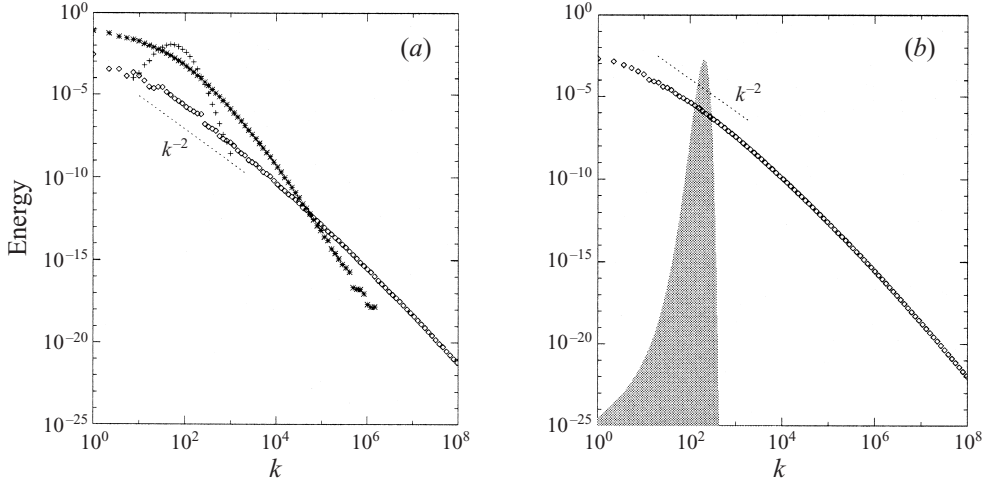
FIGURE 1. Energy spectrum of decaying turbulence: (*a*) with initial spectrum concentrated at $k = q_0 = 100$ for three different moments of time; and (*b*) with a broad initial spectrum (the initial spectrum is shaded).

here and in the Appendix are valid only if the advection of the small scales is passive, as is assumed throughout this paper). In turbulent flow, the growth of λ is directly related to Lyapunov exponents (Chertkov *et al.* 1995). When $\lambda \gg 1$, we have $\lambda \approx 2c$. In this case, we have for $k_{min} \ll k \ll k_{max}$,

$$E(\boldsymbol{x}, k, t) = \frac{N}{2\pi\sqrt{2c}q_0}k^{-2}. \tag{3.21}$$

Note that $\lambda \approx 2c \gg 1$ corresponds to the large time $\overline{\omega}t \gg 1$ and that $k_{min} = q_0\sqrt{2c}$ and $k_{max} = q_0/\sqrt{2c}$. Summarizing, we have for the large-time asymptotics, $\lambda \approx 2c \gg 1$, in the range $q_0\sqrt{2c} \ll k \ll q_0/\sqrt{2c}$,

$$E(\boldsymbol{x}, k, t) = \frac{N}{2\pi k_{max}}k^{-2}, \tag{3.22}$$

where c is given by (3.8). Because c in general depends on the coordinate, so do k_{min}, k_{max} and E. Integration of E over the coordinate will give an average over the large-scales energy spectrum, which is, of course, also scales as k^{-2}.

In figure 1(*a*) we show the energy spectrum evolution obtained by numerical integration of (2.15) with initial conditions (3.1) and random initial conditions for the large-scale flow. We see that the spectrum is indeed approaching k^{-2} shape in a growing range centred at q_0.

3.2. *The case of a finite-width initial spectrum*

As we have already mentioned, the generalization to any isotropic initial spectrum $|\hat{\omega}_0(q_0)|^2$ (and/or arbitrary isotropic pumping) is obtained by simply integrating E_k over q_0. For example, in the decaying case

$$E_k = \int \frac{|\hat{\omega}_0(q_0)|^2}{2\pi k^3 \sqrt{2cq_0^2/k^2 - q_0^4/k^4 - 1}}\, \mathrm{d}q_0. \tag{3.23}$$

It is easy to see that if the width of $|\hat{\omega}_0(q_0)|$ is of order of q_0 then the result for the k^{-2} energy spectrum scaling remains valid. Instead of (3.22) we have

$$E(\boldsymbol{x}, k, t) = C\, k^{-2}, \tag{3.24}$$

where

$$C = \frac{1}{2\pi\sqrt{2c}} \int \frac{|\hat{\omega}_0(q_0)|^2}{q_0}\, \mathrm{d}q_0. \tag{3.25}$$

Numerical simulation of (2.15) with a finite-width initial spectrum confirms that the energy spectrum behaves as k^{-2} for large time, as shown in figure 1(b).

4. Forced turbulence

Suppose first that the enstrophy is injected at $q = q_0$ at the rate σ per unit time. Because the problem is linear, the total spectrum is equal to the sum of the contributions produced by $\sigma\, \mathrm{d}t'$ injected at different moments $t - t'$,

$$E(\boldsymbol{x}, k) = \frac{\sigma}{2\pi k^3} \int_{t_c}^{\infty} \frac{\mathrm{d}t'}{\sqrt{2c(t')q_0^2/k^2 - q_0^4/k^4 - 1}}. \tag{4.1}$$

Here t_c is the minimal time required for the ellipse to reach k. Depending on whether $k < q_0$ or $k > q_0$, at $t = t_c$ we have $k = k_{min}$ or $k = k_{max}$ correspondingly. In both cases the denominator in (4.1) becomes zero, which gives a condition for finding t_c,

$$c(t_c) = \tfrac{1}{2}(q_0^2/k^2 + k^2/q_0^2). \tag{4.2}$$

4.1. Turbulence strained between vortices

Uniform straining results in an exponential growth of the ellipse aspect ratios, $\lambda = \exp(2\alpha t)$, where α is the strain rate, see the Appendix. Then, the integral in (4.1) converges and the stationary spectrum is possible. Let us find the stationary spectrum for the scales far from the pumping scale, $k \ll q_0$ and $k \gg q_0$.

4.1.1. Pure energy flux case, $k \ll q_0$

If $k \ll q_0$, the main contribution to the integral (4.1) comes from t' such that $2c \sim q_0/k \gg 1$. Then $2c = \lambda = \exp(2\alpha t) \gg 1$ and $c\,(= \tfrac{1}{2}\pi)$, and (4.1) becomes

$$\begin{aligned}
E(\boldsymbol{x}, k) &= \frac{\sigma}{k^2 q_0} \int_{t_c}^{\infty} \frac{\mathrm{d}t'}{\sqrt{\exp(2\alpha t') - q_0^2/k^2}} \\
&= \frac{\sigma}{\alpha k q_0^2} \int_0^1 \frac{\mathrm{d}z}{\sqrt{1 - z^2}} = \frac{\sigma}{\alpha k q_0^2} \arcsin x|_0^1 = \frac{\pi\sigma}{2\alpha q_0^2} k^{-1},
\end{aligned} \tag{4.3}$$

where $z = q_0 \mathrm{e}^{-\alpha t}/k$. Thus, the energy spectrum at $k \ll q_0$ has the following power-law scaling:

$$E \propto k^{-1}. \tag{4.4}$$

As we discussed before, in the freely decaying case most of the initial energy is transferred to $k \ll q_0$ when $\lambda \gg 1$ and most of the enstrophy (number of particles) to the $k \ll q_0$ range. Therefore, spectrum (4.4) corresponds to the pure energy flux. As we show in the next section, this spectrum can be derived from dimensional analysis and is, therefore, more general than just a solution in a special case of uniform strain.

4.1.2. *Pure enstrophy flux case, $k \gg q_0$*

If $k \gg q_0$, the main contribution to the integral (4.1) also comes from the $2c \sim q_0/k \gg 1$ range. In this case, (4.1) can be rewritten as

$$E(\boldsymbol{x}, k) = \frac{\sigma}{k^3} \int_{t_c}^{\infty} \frac{\mathrm{d}t'}{\sqrt{\exp\left(2\alpha t'\right) q_0^2/k^2 - 1}}$$

$$= \frac{\sigma}{\alpha k^3} \int_0^1 \frac{\mathrm{d}z}{\sqrt{1 - z^2}} = \frac{\sigma}{\alpha k^3} \arcsin x|_0^1 = \frac{\pi \sigma}{2\alpha} k^{-3}, \tag{4.5}$$

where $z = k\mathrm{e}^{-\alpha t}/q_0$. Thus, we have the following scaling for the spectrum in the $k \gg q_0$ range which corresponds to a pure enstrophy flux:

$$E \propto k^{-3}. \tag{4.6}$$

This spectrum will also be found using a dimensional argument in the next section.

4.2. *Turbulence when there is vortex-core shear*

As shown in the Appendix, vortex-core shearing results in an algebraic growth of the ellipse aspect ratios, asymptotically $\lambda = (\beta t)^2$, where β is the shear. Substituting $c = \lambda/2$ (for large λ), we have

$$E(\boldsymbol{x}, k, t) = \frac{\sigma}{k^3} \int_{t_c}^{\infty} \frac{\mathrm{d}t'}{\sqrt{(\beta t')^2 q_0^2/k^2 - q_0^4/k^4 - 1}}. \tag{4.7}$$

One can see that this integral diverges at $-\infty$. Therefore, no stationary spectrum is possible for the small-scale turbulence inside the vortex cores in our model. The physical explanation of this effect is that the line elements are stretched only linearly in time which is much slower than an exponential stretching by strain. As a result, the spectral flux induced by shearing inside the vortex core is insufficient to take turbulence away from the forcing scale fast enough for a stationary state to exist. The nonlinear interaction of small scales among themselves (ignored in this paper) acts to accelerate the spectral transfer necessary for a stationary state, but the tendency of deceleration of the spectral fluxes inside vortex cores persists. McWilliams suggested that the suppression of the enstrophy flux inside the coherent vortices is the reason for the spectra steeper than k^{-3} observed numerically (McWilliams 1984, 1990). The results of this section show that this is indeed the case for the *non-local* turbulence in a vortex core. On the other hand, the k^{-3}-spectrum is expected when turbulence is not trapped in vortex cores so that the spectral fluxes can quickly be developed when the turbulence gets between vortices. We will discuss our numerical results for the case of forced turbulence in §4.4.

4.3. *The case of a broad-band forcing*

Suppose now that turbulence is forced over a range of wavenumbers which is of the same order as the wavenumber itself and that the vorticity generated per unit time in the interval $\mathrm{d}q_0$ is $\zeta(q_0) \mathrm{d}q_0$. Then instead of (4.1) we have

$$E(\boldsymbol{x}, k) = \frac{1}{2\pi k^3} \int \zeta(q_0) \mathrm{d}q_0 \int_{t_c}^{\infty} \frac{\mathrm{d}t'}{\sqrt{2c(t') q_0^2/k^2 - q_0^4/k^4 - 1}}. \tag{4.8}$$

For $k \ll q_0$ (where q_0 is the characteristic forcing wavenumber), we have instead of (4.3)

$$E(\boldsymbol{x}, k) = \frac{\pi}{2\alpha} \left(\int \frac{\zeta \, \mathrm{d}q_0}{q_0^2} \right) k^{-1}. \tag{4.9}$$
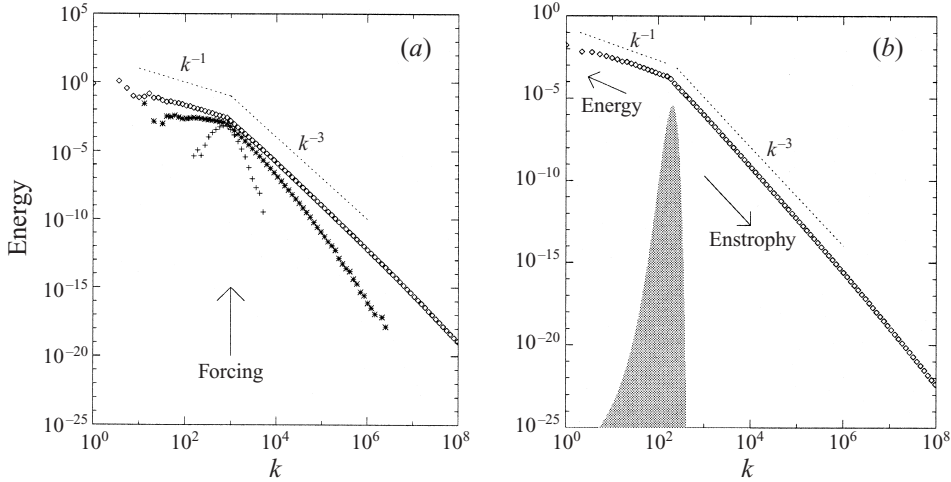
FIGURE 2. Energy spectrum of small-scale turbulence: (a) forced at a single wavenumber, and (b) forced in a finite wavenumber range (the forcing shape is shaded).

For $k \gg q_0$, expression (4.5) will be replaced with

$$E(\boldsymbol{x}, k) = \frac{\pi}{2\alpha} \left(\int \zeta \, \mathrm{d} q_0 \right) k^{-3}. \tag{4.10}$$

4.4. Numerical results for forced turbulence

In the case of forced turbulence the numerical computations serve a greater purpose than just illustrating the analytical results. Indeed, the theory predicts different behaviour (1) for forced turbulence in vortex cores and (2) for turbulence between vortices. Thus, it is not clear *a priori* what type of behaviour is dominating in the general case, in particular when the large scales are initially random. In figures 2(a) and 2(b), we show the numerical results for the energy spectrum of small-scale turbulence with a narrow- and a broad-band forcing respectively. In both cases, the large-scale flow was random initially. Stationary k^{-1}- and k^{-3}-spectra are clearly seen at large time. This means that turbulence straining between vortices is the main dynamical process dominating the turbulence evolution. Using a pictorial interpretation of Chertkov *et al.* (1995), one could say that the 'sea of strain' dominates the 'islands of vorticity'. On the other hand, we do observe a spectrum steeper than k^{-3} for small turbulent regions inside intense vortices. In figure 3 we show a typical large-scale vorticity distribution and an intense vortex marked by the dashed line which is a vorticity contour at ten times the average vorticity value. The energy spectrum of small-scale turbulence measured in such a vortex is shown in figure 4. One can see that this spectrum is closer to k^{-4} than to k^{-3}.

5. Dimensional analysis for the non-local energy and enstrophy cascades

In the non-local case, the interaction among the small scales is negligible compared with interaction via large scales. Corresponding equations for the small-scale turbulent spectrum are linear with a characteristic time determined by the large-scale strain and/or shear. Further, these equations have the form of a conservation law for the small-scale enstrophy (number of particles) and, therefore, there is no enstrophy
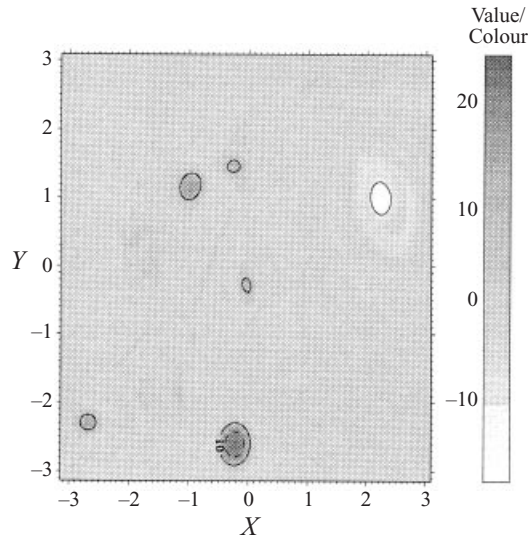
FIGURE 3. Large-scale vorticity. The intense vorticity regions are marked by contours.
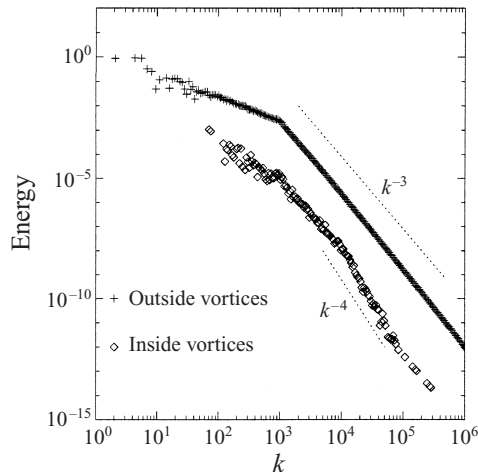

FIGURE 4. Energy spectrum of small-scale turbulence inside and outside of the intense vortices.

transfer between the small and large scales. A more subtle fact is that the small-scale energy is also conserved if the initial small-scale spectrum is isotropic (Nazarenko *et al.* 1999). The enstrophy transfer between the small scales is much more local in non-local turbulence than in local turbulence. This, at first sight paradoxical, statement is valid because any interacting wavenumber triad contains one small wavenumber (large scale) and two large wavenumbers with very close values (small scales), and the enstrophy is transferred only between these large wavenumbers. Recall that in local turbulence all wavenumbers are similar in the interacting triad, and the enstrophy transfer takes place between *similar* but not *nearly equal* wavenumbers. On the other hand, the energy transfer is less local (it is as local as, perhaps, in local turbulence) because for each individual triad the small-scale energy is not conserved (only the total energy of all triads is conserved for isotropic initial spectra).

In stationary turbulence the enstrophy and energy fluxes are constant. As in local turbulence, the enstrophy cascade is directed toward large k and the energy cascade is inverse, i.e. toward smaller k with respect to the pumping scale q_0. Indeed, if a finite enstrophy dissipation at $k \ll q_0$ were to imply an infinite energy dissipation at these scales, and, in turn, a finite energy dissipation at $k \gg q_0$ would mean an infinite enstrophy dissipation there. This standard reasoning to find the directions of the enstrophy and energy fluxes is independent of the locality (or non-locality) assumption. However, Kraichnan's (1967) dimensional derivation of the energy spectra, corresponding to the enstrophy and energy cascades, does rely on locality. Below we shall see the consequences of this fact for the energy spectrum exponents.

Consider first $k \ll q_0$ where the enstrophy flux η is negligible and the shape of the energy spectrum is determined by the energy flux ϵ. The energy flux ϵ has dimension l^2/t^3 and the large-scale flow is characterized by the rate of strain α that has the dimension $1/t$. Because the equations are linear, the energy spectrum must be linear in ϵ. The only combination of ϵ, α and $k \sim 1/l$ that has the dimension l^3/t^2 of the energy spectrum and is linear in ϵ is

$$E_k \propto \frac{\epsilon}{\alpha} k^{-1}. \tag{5.1}$$

Thus, we see that the energy cascade is characterized by a -1 spectral exponent in non-local turbulence, which is different from the famous $-5/3$ valid for local turbulence. This spectrum coincides with the exact analytical solution obtained above for $k \ll q_0$ for the special case of uniform large-scale strain.

Now let us consider $k \gg q_0$ where the energy spectrum is determined by the enstrophy flux η having dimension $1/t^3$. The only combination of η, α and $k \sim 1/l$ that has the dimension of the energy spectrum and is linear in η is

$$E_k \propto \frac{\eta}{\alpha} k^{-3}. \tag{5.2}$$

This spectrum coincides with the exact analytical solution obtained above for $k \gg q_0$ for the special case of uniform large-scale strain.

As we see, the spectral exponent -3 is the same for local and non-local turbulence. This arises because the dimension of the enstrophy flux does not involve l, and the way we match the temporal part in the dimension of E_k ($\eta^{2/3}$ for local turbulence or η/α for non-local turbulence) does not change the spatial scale dependence k^{-3}.

Note that the dimensional argument presented in this section does not rely on the two-dimensionality of the system and it is valid also for three-dimensional turbulence if the latter is non-local. Nonlocality does not arise naturally in three-dimensions because there is no inverse cascade and energy condensation in large scales in this case. However, non-locality can be induced externally by a mean shear, e.g. in a turbulent channel flow.

6. Passive scalar spectra

As we have mentioned in the Introduction, the dynamics of vorticity in non-local two-dimensional turbulence is identical to the dynamics of a small-scale passive-scalar concentration field $n(x, t)$ advected by a large-scale velocity field u. In this section, we apply the results obtained above for two-dimensional turbulence to the passive-scalar advection problem. We consider Batchelor's regime for the passive-scalar when its scale is much smaller than that of the advecting velocity field. The passive scalar

spectrum is defined as

$$P(\pmb{x}, k, t) = 2\pi \int |\hat{n}(\pmb{x}, \pmb{k}, t)|^2 \, k \, \mathrm{d}\theta, \tag{6.1}$$

where θ is the polar angle in the wavenumber space and $\hat{n}$ is the Gabor transform of n,

$$\hat{n}(\pmb{x}, \pmb{k}, t) = \int f(\epsilon^* |\pmb{x} - \pmb{x}_0|) \mathrm{e}^{i\pmb{k} \cdot (\pmb{x} - \pmb{x}_0)} n(\pmb{x}_0, t) \, \mathrm{d}\pmb{x}_0 \tag{6.2}$$

(see (2.3) for notation). The scalar variance is equal to $\int P \, \mathrm{d}k \, \mathrm{d}\pmb{x}$ if f satisfies normalization condition $\int f^2(\epsilon^* |\pmb{x} - \pmb{x}_0|) \, \mathrm{d}\pmb{x}_0 = 1$. (Note an analogy with the definition of the passive scalar spectrum in terms of the Fourier transforms in such a way that its integral over k is equal to the variance.)

6.1. *Pseudo-energy*

One obvious conservation law for the passive scalar, which is analogous to the enstrophy conservation in two-dimensional turbulence, is

$$\Pi_t + \pmb{u} \cdot \nabla \Pi = 0, \tag{6.3}$$

where

$$\Pi(\pmb{x}, t) = \int P \, \mathrm{d}k. \tag{6.4}$$

Remarkably there is also an analogue of the energy conservation in the case when the passive scalar spectrum is initially isotropic,

$$I_t + \pmb{u} \cdot \nabla I = 0, \tag{6.5}$$

where

$$I(\pmb{x}, t) = \int \frac{|\hat{n}(\pmb{x}, \pmb{k}, t)|^2}{k^2} \, \mathrm{d}k. \tag{6.6}$$

Indeed, by substituting

$$\hat{n}(\pmb{x}, \pmb{k}, t) = \hat{n}(\pmb{a}, \pmb{q}, 0) \tag{6.7}$$

and (2.12) in (6.6), changing the variable of integration to $\pmb{q}$ and taking into account that $\det \Lambda = 1$, we obtain that I depends on $\pmb{x}$ and t only via $\pmb{a}(\pmb{x}, t)$. But this means that I satisfies equation (6.5). Keeping in mind the turbulence analogy, we will call invariant I the pseudo-energy.

It is easy to generalize this result to an arbitrary number of dimensions D, in which case the invariant of pseudo-energy is

$$I(\pmb{x}, t) = \int \frac{|\hat{n}(\pmb{x}, \pmb{k}, t)|^2}{k^D} \, \mathrm{d}\pmb{k}. \tag{6.8}$$

To prove this let us assume that the initial passive scalar spectrum is isotropic,

$$I(\pmb{x}, t) = |\hat{n}(\pmb{x}, \pmb{k}, t)|^2 = |\hat{n}(\pmb{a}, \pmb{q}, 0)|^2 = f(\pmb{a}, q), \tag{6.9}$$

where $q = |\pmb{q}|$ and $f(\pmb{a}, q)$ is an arbitrary function which is zero at $q = 0$ and $q \to \infty$. Denoting $A = (\Lambda^T)^{-1}$ we have

$$(\partial_t I)_{\pmb{a} = const} = (\partial_t)_{\pmb{a} = const} \int \frac{|f(\pmb{a}, |A\pmb{k}|)|^2}{k^D} \mathrm{d}\pmb{k}$$

$$= \int \frac{(\dot{A}\pmb{\xi}, A\pmb{\xi})}{(A\pmb{\xi}, A\pmb{\xi})} k \, \frac{\partial_k |f(\pmb{a}, |A\pmb{k}|)|^2}{k^D} \, k^{D-1} \, \mathrm{d}k \, \mathrm{d}s(\pmb{\xi}) = 0. \tag{6.10}$$
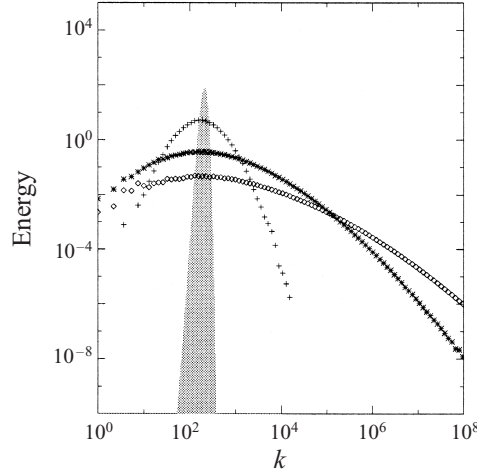
FIGURE 5. Spectrum of decaying passive scalar for three different moments of time. The initial
spectrum is shaded.

Here we used the chain rule when differentiating f and we used the spherical variables
$k = |\mathbf{k}|$ and $\boldsymbol{\xi} = \mathbf{k}/k$ with $\mathrm{d}s(\boldsymbol{\xi})$ being the infinitesimal surface element on the unit
sphere $k = 1$. As we see, in $\mathbf{a}, t$ variables I is independent of time which means that
it is a Lagrangian invariant.

Note that the pseudo-energy is conserved only when the passive scalar scale is
much less than the scale of the advecting field. Therefore, the pseudo-energy is an
adiabatic invariant rather than an exact one.

6.2. *Free decay in two dimensions*

To obtain the passive scalar spectra one can just divide the energy spectra obtained
for two-dimensional turbulence by k^2. For a freely decaying (i.e. unforced) passive
scalar spectrum then it follows from (3.23) that

$$P_k = \int \frac{|\hat{n}_0(q_0)|^2}{2\pi k \sqrt{2cq_0^2/k^2 - q_0^4/k^4 - 1}} \, \mathrm{d}q_0, \tag{6.11}$$

where $\hat{n}_0$ is the initial spectrum. In the case $c \sim u\,t/L \gg 1$ we have for $k_{min} \ll k \ll k_{max}$,

$$P(\mathbf{x}, k, t) = C\,k^0, \tag{6.12}$$

where

$$C = \frac{1}{2\pi\sqrt{2c}} \int \frac{|\hat{n}_0(q_0)|^2}{q_0} \, \mathrm{d}q_0. \tag{6.13}$$

A numerically obtained spectrum of freely decaying passive scalar is shown in
figure 5. As predicted, the spectrum tends to a constant in an expanding range of
wavenumbers centred at the initial scale.

6.3. *Forced two-dimensional passive scalar*

Suppose that a passive scalar is forced so that the passive scalar generated per unit
time in the interval $\mathrm{d}q_0$ is $\xi(q_0)\,\mathrm{d}q_0$. It follows from the analysis of two-dimensional
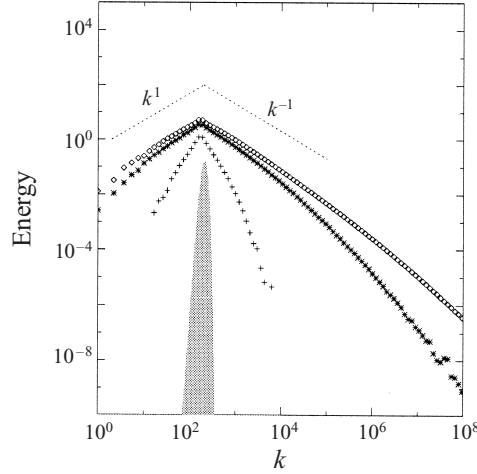turbulence that no stationary passive scalar spectrum is possible inside the vortex

FIGURE 6. Forced passive scalar spectrum for three different moments of time. The shape of the forcing is shaded.

cores of the advecting velocity field, whereas between the vortices we have from (4.8)

$$P(\boldsymbol{x}, k) = \frac{1}{2\pi k} \int \xi(q_0) \, dq_0 \int_{t_c}^{\infty} \frac{dt'}{\sqrt{2c(t')q_0^2/k^2 - q_0^4/k^4 - 1}}. \qquad (6.14)$$

Consider the uniform strain flow, $\boldsymbol{u} = (\alpha x, -\alpha y)$. For $k \gg q_0$ (where q_0 is the characteristic forcing wavenumber), we obtain the famous Batchelor's k^{-1}-spectrum,

$$P(\boldsymbol{x}, k) = \frac{\pi}{2\alpha} \left(\int \xi \, dq_0 \right) k^{-1}. \qquad (6.15)$$

This spectrum corresponds to the constant spectral flux of the passive scalar toward high wavenumbers.

For $k \ll q_0$ we have

$$P(\boldsymbol{x}, k) = \frac{\pi}{2\alpha} \left(\int \frac{\xi \, dq_0}{q_0^2} \right) k^1. \qquad (6.16)$$

This spectrum corresponds to the constant spectral flux of the pseudo-energy I. It will be considered in greater detail in the next section.

In figure 6, we show the spectrum of the forced passive scalar advected by a random-field large-scale flow. One can see that Batchelor's k^{-1}-spectrum is formed on the high-wavenumber side of the forcing scale, whereas the k^1-spectrum is seen on the low-k side of the forcing.

6.4. *Pseudo-energy cascade in a higher number of dimensions*

The k^1-spectrum is, in fact, a $D = 2$ version of the k^{D-1}-spectrum obtained by Kraichnan (1974). Because the pseudo-energy invariant was not known, the importance of this spectrum as a cascade-type spectrum was not understood, and it was misinterpreted as corresponding to an absolute statistical equilibrium state. Let us consider the equation for the passive scalar spectrum derived by Kraichnan for the case of a velocity field, δ-correlated in time and write a zero-diffusion limit of this equation,

$$\partial_t F = C[k\partial_{kk} - (D-1)\partial_k](kF), \qquad (6.17)$$

where F is the passive scalar spectrum averaged over the large scales and C is a coefficient determined by the mean advection. Equation (6.17) can be also rewritten as

$$\partial_t F = \partial_k (Ck^{D+1}\partial_k(k^{1-D}F)), \qquad (6.18)$$

which is a continuity equation expressing conservation of the passive scalar. The power-law solution that corresponds to the constant passive scalar flux is, as is well-known, $F \propto k^{-1}$.

On the other hand, one can re-write (6.17) in the form of yet another conservation law via multiplying it by k^{-D},

$$\partial_t(F/k^D) = \partial_k[Ck^{1-D}\partial_k(kF)]. \qquad (6.19)$$

Thus,

$$\int_0^\infty \frac{F}{k^D} \, dk = \text{const}, \qquad (6.20)$$

which expresses the pseudo-energy conservation in the D-dimensional case. It is a special case of the conservation law (6.10) which was obtained without the assumption that the velocity field is δ-correlated in time. According to (6.19), the flux of the pseudo-energy (6.20) is $Ck^{1-D}\partial_k(kF)$, and the constant-flux solution satisfies

$$Ck^{1-D}\partial_k(kF) = \text{const},$$

which gives

$$F \propto k^{D-1}.$$

This spectrum corresponds to an equipartition of the passive scalar in the phase space. However, it corresponds to a state which is very far from an absolute statistical equilibrium, because there is an inverse cascade of the pseudo-energy associated with this solution. Moreover, it is easy to see that the pseudo-energy invariant is equipartitioned in k-space on the k^{-1}-spectrum. Therefore, the situation is completely symmetric for the k^{D-1}- and k^{-1}-spectra in that both of them correspond to a constant cascade of one invariant and, simultaneously, to an equipartition of another integral of motion.

7. Conclusion

A semi-classical description based on using the Gabor transform proved to be an efficient tool for studying non-local two-dimensional turbulence and passive scalar turbulence in Batchelor's regime. It allows variations in the small-scale dynamics depending on the local large-scale flow to be described. For example, it allowed the fact that the turbulence spectra are steeper inside the vortex cores than between vortices to be established. This is supported by two analytical solutions obtained for the cases of a pure stationary strain and a stationary round vortex and it is also confirmed by numerical simulations. Note that numerical simulations serve a more important role in this case than just an illustration of the analytical results because in turbulence the shear and strain are not stationary and the vorticity (or scalar) elements may not have enough time to align. Numerical simulation of the semi-classical equations by the PIC method allows one to work with very large inertial intervals, typically eight decades wide. Cascade-type spectra and spectra of decaying turbulence can be obtained within the semi-classical description analytically for a general form of the large-scale flow without using averaging over large scales. It is natural to think that two-dimensional turbulence becomes non-local for large time because of the energy
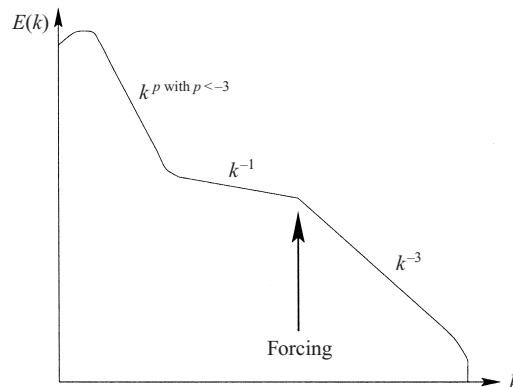
FIGURE 7. Expected spectrum of forced turbulence for large time in the case when the forcing scale and the largest scale of the system are well separated.

condensation at the largest scale. If this is true, then for very large time one should expect the spectrum of forced turbulence to be as shown in figure 7.

Note that the k^{-1}-spectrum will be observed only if the forcing scale is much less than the largest scale of the system. When approaching the largest scale, the non-local inverse energy flux 'slows down' and changes spectral slope from -1 to a sharper one corresponding to the energy condensate. It is important to understand that the k^{-1}-spectrum will only be observed for non-local turbulence whereas the k^{-3} enstrophy cascade is not sensitive to the non-locality property as it is the same for both local and non-local turbulence. Thus, the picture suggested on figure 7 should be considered as a hypothesis which is valid if the slope of the large-scale condensate gets steeper than -3 (condition of nonlocality of the small-scale turbulence). Unfortunately, it is at present impossible to test the hypothesis of non-locality using direct numerical simulations, because of insufficient resolution and the large required time for simulations. On the other hand, it is possible to compute the entire spectrum by treating the small-scale turbulence and large-scale condensate as two different fluids. Because there is no spectral gap in this case, the large-scale component may leak into the small scales and the low-k tail of the small-scale component may start overlapping with the large scales. Thus, one has to implement a procedure to transfer the large-scale component into the small-scale one and back when they cross a wavenumber k_b taken to be a boundary separating the large and small scales. As in this paper, the small-scale component can be computed by the PIC code, whereas the pseudo-spectral method can be used for the large-scale component. In this case, the natural choice for k_b is given by the smallest scale of the pseudo-spectral scheme. Numerical results obtained by such a two-fluid numerical method are reported in Laval *et al.* (1999).

It is interesting that the k^{-1}-spectrum is observed experimentally in near-wall turbulence by Perry, Henbest & Chong (1986). The near-wall turbulence is, of course not two-dimensional, but it is likely to be very non-local in that the turbulence interaction with the large-scale mean flow dominates its dynamics. Thus, the k^{-1}-spectrum in this case may have a similar origin, especially considering that the dimensional argument presented in §5 is independent of the number of dimensions.

One remark should be made about the non-locality in the direct cascade of enstrophy. It is known that equal intervals of the k^{-3} spectrum give equal contributions to the enstrophy transfer (Kraichnan 1971). In the present paper, these contributions have been assumed to be small compared to the enstrophy transfer via straining

the large-scale component. Naturally, for very high wavenumbers this assumption will fail, and the small-scale k^{-3}-spectrum itself will start dominating the enstrophy transfer (G. Eyink 1998, personal communication). Such a transfer is also non-local, but in a different way from that considered in this paper. This regime was considered by Kraichnan (1971) who showed that one should expect a logarithmic correction to the k^{-3}-spectrum in this case.

We thank Professor Babiano for help with numerics and useful discussions.

Appendix A. Evolution of the ellipse aspect ratio in straining and shearing large-scale flows

We will consider two special cases of large-scale flows: an axially symmetric vortex and a uniform strain flow. These two examples correspond to the characteristic behaviour on the 'islands of vorticity' and in the 'sea of strain' in a general turbulent flow (Chertkov *et al.* 1995).

A.1. *Axially symmetric vortex*

Let us solve the ray equations (2.9) and (2.10) for the case of an axisymmertic vortex when $\bar{\boldsymbol{u}} = U(r)\boldsymbol{e}_\phi$, where r and ϕ are the polar coordinates, and $\boldsymbol{e}_\phi$ is a unit vector tangent to $r = $ const. Here, the velocity profile $U(r)$ is arbitrary, provided it is large scale and satisfies the condition (2.2). The solution of (2.9) in this case is just a uniform rotation,

$$r = \text{const}, \tag{A 1}$$

$$\phi = \Omega t + \phi_0, \tag{A 2}$$

where $\Omega = U/r$ is the angular velocity. For the wavenumber we have

$$\dot{k}_r = \Omega k_\phi - k_\phi \partial_r U, \tag{A 3}$$

$$\dot{k}_\phi = -\Omega k_r + \frac{1}{r}k_r U = 0. \tag{A 4}$$

Solving these equations, we obtain

$$k_\phi = \text{const} = q_{\phi 0}, \tag{A 5}$$

$$k_r = -q_{\phi 0}r\beta t + q_{r0} \tag{A 6}$$

where $\beta = r\partial_r\Omega$. Near the vortex centre $\partial_r\Omega = 0$ and $k_r = $ const. so that the wavevector is just uniformly rotating without any change in magnitude. For large time, $r\beta t \gg 1$, the initial ring $k = q_0$ becomes an ellipse with

$$k_{max} \approx q_0|\beta|t, \tag{A 7}$$

$$k_{min} = q_0^2/k_{max} \approx q_0/|\beta|t, \tag{A 8}$$

$$\lambda = k_{max}/k_{min} \approx (\beta t)^2. \tag{A 9}$$

A.1.1. *Uniform strain flow*

For uniform strain flow, the large-scale velocity field is $\bar{\boldsymbol{u}} = (U_x, U_y)$ with

$$U_x = \alpha x, \tag{A 10}$$

$$U_y = -\alpha y, \tag{A 11}$$

where the x- and y-axes are chosen to be principal axes of the strain, and $\alpha = \text{const}$. In this case,

$$\dot{k}_x = -\alpha k_x, \tag{A 12}$$

$$\dot{k}_y = \alpha k_y. \tag{A 13}$$

Solving these equations, we have

$$k_x = q_{0x} \exp(-\alpha t), \tag{A 14}$$

$$k_y = q_{0y} \exp(\alpha t). \tag{A 15}$$

For large time, $\alpha t \gg 1$, we have the following ellipse parameters:

$$k_{max} \approx q_0 \exp(\alpha t), \tag{A 16}$$
$$k_{min} \approx q_0 \exp(-\alpha t), \tag{A 17}$$
$$\lambda \approx \exp(2\alpha t). \tag{A 18}$$

REFERENCES

BABIANO, A., BASDEVANT, C., LEGRAS, B. & SADOURNY, R. 1987 *J. Fluid Mech.* **183**, 379.

BATCHELOR, G. K. 1959 *J. Fluid Mech.* **5**, 113.

BENZI, R., PALADIN, G., PATARNELLO, S., SATANGELO, P. & VULPIANI, A. 1986 *J. Phys.* A: *Math. Gen.* **19**, 3771.

BENZI, R., PATNELLO, S. & SANTANGELO, P. 1987 *Europhys. Lett.* **3**, 811.

BORUE, V. 1993 *Phys. Rev. Lett.* **71**, 3967.

BORUE, V. 1994 *Phys. Rev. Lett.* **72**, 1475.

BRACHET, M. E., MENGUZZI, M. & SULEM, P. L. 1986 *Phys. Rev. Lett.* **57**, 683.

BRACHET, M. E., MENGUZZI, M., POLITANO, H. & SULEM, P. L. 1988 *J. Fluid Mech.* **194**, 1988.

CARDOSO, O., MARTEAU, D. & TABELING, P. 1994 *Phys. Rev.* E **49**, 454.

MARTEAU, D., CARDOSO, O. & TABELING, P. 1995 *Phys. Rev.* E **51**, 5124.

CHERTKOV, M., FALKOVICH, G., KOLOKOLOV, I. & LEBEDEV, V. 1995 *Phys. Rev.* E **51**, 5609.

COUDER, Y. 1984 *J. Phys. Lett.* **45**, 353.

DUBRULLE, B. & NAZARENKO, S. V. 1997 *Physica D* **110**, 123.

DYACHENKO, A. I., NAZARENKO, S. V. & ZAKHAROV, V. E. 1992 *Phys. Lett.* A **165**, 330.

KEVLAHAN, N. K.-R. & FARGE, M. 1997 *J. Fluid Mech.* **346**, 1997.

KRAICHNAN, R. H. 1967 *Phys. Fluids* **10**, 1417.

KRAICHNAN, R. H. 1971 *J. Fluid Mech.* **47**, 525.

KRAICHNAN, R. H. 1974 *J. Fluid Mech.* **64**, 737.

KRAICHNAN, R. H. 1975 *J. Fluid Mech.* **67**, 155.

LAVAL, J.-P., DUBRULLE, B. & NAZARENKO, S. V. 1999 Dynamical modelling of sub-grid scales in two-dimensional turbulence, *Physica D* (submitted).

MCWILLIAMS, J. C. 1984 *J. Fluid Mech.* **146**, 21.

MCWILLIAMS, J. C. 1990 *Phys. Fluids* A **2**, 547.

NAZARENKO, S. V., KEVLAHAN, N. & DUBRULLE, B. 1999 *J. Fluid Mech.* **390**, 325.

NAZARENKO, S. V., ZABUSKY, N. J. & SCHEIDEGGER, T. 1995 *Phys. Fluids* **7**, 2407.

OHKITANI, K. 1991 *Phys. Fluids* A **3**, 1598.

PERRY, A. E., HENBEST, S. & CHONG, M. S. 1986 *J. Fluid Mech.* **165**, 163.

SANTANGELO, P., BENZI, R. & LEGRAS, B. 1989 *Phys. Fluids* A **1**, 1027.

SMITH, L. & YAKHOT, V. 1993 *Phys. Rev. Lett.* **71**, 352.

SOMMERIA, J. 1985 PhD thesis.

WEISS, J. 1991 *Physica D* **48**, 273.